



Efficient drilling of amorphous alloy foils using low-energy long pulses of a Nd:YAG laser

Takeshi Tsuji^{1,2} · Shota Yamamoto¹ · Shun Ikemoto¹ · Hiromasa Hara¹ · Motoki Ohta² · Daisuke Nakamura³

Received: 3 January 2022 / Accepted: 8 March 2022 / Published online: 14 March 2022
© The Author(s), under exclusive licence to Springer-Verlag London Ltd., part of Springer Nature 2022

Abstract

Laser drilling of amorphous alloy foils was conducted using low-energy long pulses (LP) generated using a Nd:YAG laser. Results showed that LP can drill an amorphous alloy foil more efficiently than a nanosecond pulse (NSP) can: An LP at 1 mJ can open a through-hole on an amorphous alloy foil with 25 μm thickness although a single-shot NSP at 20 mJ formed a crater with ca. 3 μm depth. From these findings, we infer that the markedly higher drilling efficiency of a low-energy LP than that of NSP is attributable to 1) lower plasma generation by LP than by NSP, and 2) continuous heating of the target material by multiple sub-pulses in an LP. Results also demonstrate that low-energy LP drilling is applicable to various metal foils and that the drilling efficiency depends on the metal species. The results of the analysis of the relation between some physical properties of the metals and the drilling efficiency suggested that the drilling would proceed via melting of materials.

Keywords Laser ablation · Laser drilling · Long-pulse · Nd:YAG laser · Amorphous alloy · Metal foil

1 Introduction

Lasers can be used as powerful and versatile material machining tools. Because laser beam (particularly that of short-pulse lasers) can deposit energy at high density on materials, it can heat a limited portion of materials efficiently [1–3]. Due to this feature, lasers are particularly useful for hard materials such as amorphous alloy foils, which are ideal materials for motor core and transformers [4–9]. However, laser machining has some shortcomings compared to conventional machining techniques such as mechanical punching. The most important shortcoming must be its lower machining rate. The simplest solution to increase the machining rate is increasing the laser power. However, the increased laser power is usually accompanied by higher energy consumption, cost of facilities (laser system, optics,

protection facilities), and material degradation such as crystallization of amorphous alloys [4].

Because the major factors that decrease the laser machining rate are energy dispersion and plasma shielding, the use of short-pulse lasers such as picosecond and femtosecond lasers to suppress these effects has been regarded as another promising solution to improve efficiency [10–14]. For example, findings of earlier studies have demonstrated that a femtosecond laser at low energy (2 mJ/pulse) can drill and cut amorphous alloy efficiently, with no observed material degradation [15].

Although the use of femtosecond lasers is a promising solution, exploring alternative methods is important, because laser machining has many applications. In this report, we propose the use of a long pulse (LP) at low energy generated by a conventional Nd:YAG laser as an alternative method. An LP of a Nd:YAG laser is generated when a Q-switch of a nanosecond laser system is turned off. Consequently, an LP is more simply generated than a nanosecond pulse (NSP). In actuality, LPs are used widely today for medical treatments such as dental cleaning. Reportedly, laser drilling using LPs is also applicable to metals such as Al [16] and Ti [16]. Unlike an NSP, an LP comprises a series of sub-pulses with duration of several 100 ns; the range of a series is more than 100 μs , as described in the Experimental section. As inferred from such a temporal profile of an LP, the

✉ Takeshi Tsuji
tkstsuji@riko.shimane-u.ac.jp

¹ Interdisciplinary Faculty of Science and Engineering, Shimane University, Matue, Japan

² Next Generation Tatara Co-Creation Center, Shimane University, Matue, Japan

³ Graduate School of Information Science and Electrical Engineering, Kyushu University, Fukuoka, Japan

drilling efficiency of an LP is expected to be lower than that of an NSP because the heat dispersion and plasma shielding effects can increase concomitantly with increasing laser pulse duration. However, results of this study demonstrate that the drilling speed of an LP is markedly higher than that of an NSP in the 1–20 mJ/pulse range.

2 Experimental

A pulsed Nd:YAG laser system (GCR-200; Spectra-Physics KK) operated at 10 Hz was used as the laser source. The laser light wavelength was 1064 nm. This laser system can generate NSPs (8 ns width) when the Q-switch is turned on and can generate LPs when the Q-switch is turned off. Figure 1 shows the temporal profile of an LP which was obtained by detecting laser light using a photodiode (S1722-02; Hamamatsu Photonics) and a digital oscilloscope (TDS3032; Tektronix). One LP comprises 18 sub-pulses of which the width and interval are, respectively, ca. 400 ns and 3–7 μ s. Its total pulse width is ca. 100 μ s. Figure 2 portrays spatial profiles of an NSP and that of an LP. These curves were obtained conventionally by measuring the energy of the laser beam transmitted through an iris of which center position was adjusted at the center of the laser beam, while changing the iris diameter. No significant difference was found between the profile of an NSP and that of an LP. Both pulses have a Gaussian-like intensity distribution.

Metglas® (2605HB1M of component, Fe-Si-B, ca. 1420–1470 K melting point, $7.74 \text{ W m}^{-1} \text{ K}^{-1}$ thermal conductivity, $7.33 \times 10^3 \text{ kg/m}^3$ density, 25 μ m thickness; Hitachi Metal Ltd.) was used as the amorphous alloy foil for which laser drilling was applied. After a piece of foil was set on a motorized stage, a laser beam was focused on the foil through a convex lens ($f = 100 \text{ mm}$). The focal point was

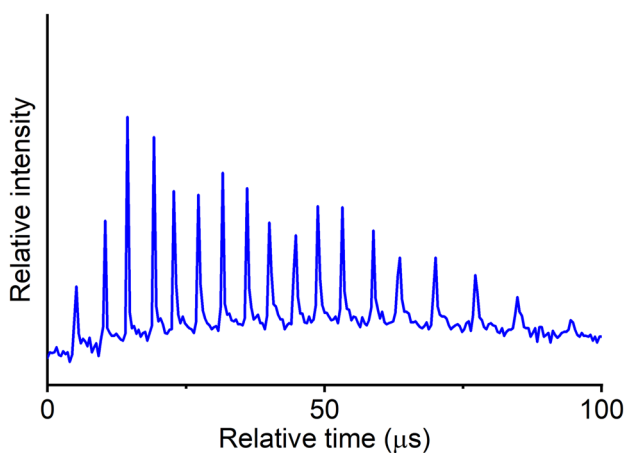


Fig. 1 Temporal profile of an LP generated by the Nd:YAG laser used in this study

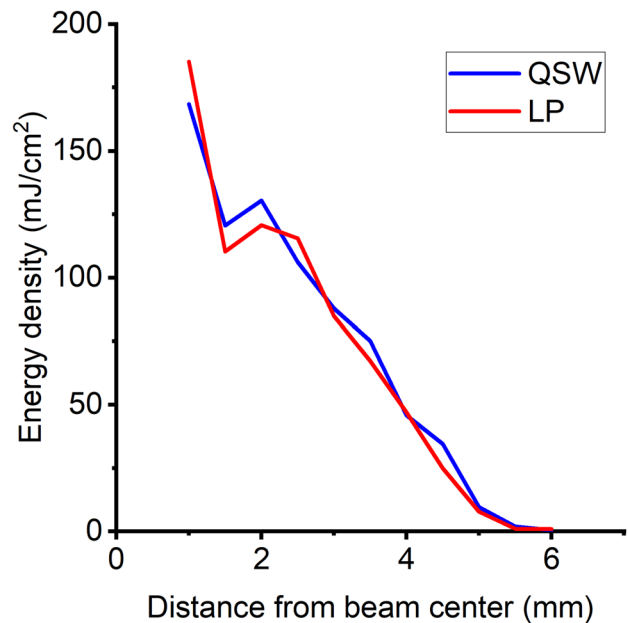


Fig. 2 Spatial profiles of an NSP and an LP generated by the Nd:YAG laser used in this study

adjusted to minimize the diameter of the craters or holes formed on the foil. The motorized stage was scanned at 2000 mm/s during laser irradiation to avoid overlapping of holes or craters. The same procedure was also used when laser irradiation was conducted for foils of Ag, Al, Au, Cu, Mo, Nb, Ni, Pt, W, and Zn purchased from the Nilaco Corp. The thickness and some thermal properties of these foils are presented in Table 1. The morphology and depth profiles of the craters and holes formed on the foils were observed, respectively, using SEM (JCM-6000Plus; JEOL) and a three-dimensional optical interferometer (VS1800; Hitachi High-Technologies Corp.).

The optical emission spectra of laser-generated plasma were observed with a multichannel spectrometer (PMA-10; Hamamatsu Photonics KK) that had been synchronized with the laser system. The observation of time-resolved photographs of the laser ablation process was conducted using a high-speed camera (FASTCAM SA-X2; Photron Ltd.), which was operated at a frame rate of 540,000 frame/s with a shutter speed of 293 ns. Details of the high-speed camera observations are presented elsewhere [17].

3 Results and discussion

3.1 Comparison of drilling efficiency between NSP and LP

Figure 3a shows an SEM image and depth profile of a crater on a Metglas foil formed using NSP at 20 mJ. The

Table 1 Physical properties of metals analyzed in the present study

Metal species	Melting point ^a (K)	Heat capacity ^a (J g ⁻¹ K ⁻¹)	Enthalpy of fusion ^a (J g ⁻¹)	Density ^a (g cm ⁻³)	Energy necessary to melt per volume at 298 K ^b (J cm ³)	Thermal conductivity at 300 K ^a (W m ⁻¹ K ⁻¹)	Thermal diffusivity at 300 K ^c (mm ² s ⁻¹)	Extinction coefficient at 1064 nm ^d
Al	933	0.897	397	2.7	2610	237	98	11.8
Cu	1356	0.385	209	9.0	5554	401	116	7.8
Mo	2883	0.251	391	10.2	10,637	138	54	5.3
Ni	1728	0.444	298	8.9	8303	90.7	23	5.5
W	3683	0.132	285	19.3	14,134	174	68	4.1
Zn	629	0.388	108	7.1	1855	113	42	5.3

^aData are cited from John Rumble ed., CRC Handbook of Chemistry and Physics, 102nd edition, CRC Press, New York, 2021

^bData were obtained by using Eq. (1)

^cData were obtained by using Eq. (2)

^dData were obtained by interpolating values listed in the above handbook

surface morphology of the foils after laser irradiation closely resembles that of similar amorphous alloy foils (Metglas@ 2605S2) shown in results of an earlier study [4]. The average depth of the craters formed by single pulse was 3 μm . The height of the debris surrounding the craters was 3 μm . To obtain a hole through the foil, about 10 pulses were necessary (Fig. 3b). The height of the debris around the hole was increased to 15 μm . No increase in the drilling efficiency was observed when laser irradiation was done using NSP at 266 nm wavelength.

Significant different results were obtained when laser irradiation was conducted using LPs. As portrayed in Fig. 4a, holes through the foil were formed by an LP at 20 mJ. In addition, through-holes were formed when the laser intensity was reduced to 1 mJ (Fig. 4b). The decrease in the diameter

of holes formed at 1 mJ is attributable to the Gaussian-like intensity distribution of the laser pulse: The intensity of the central portion of the laser beam is higher than that at the peripheral portion. The debris height around the holes was 3 μm at 1 mJ and 4–5 μm at 20 mJ, indicating that the height of the debris formed around a through-hole by an LP is lower than that formed by tens of NSPs.

To investigate the drilling depth of an LP, laser irradiation of stacked foils (30 layer) was conducted because thicker foil was unavailable. The focal point was set at the top foil. After irradiation of LPs with various amounts of energy, the number of foils for which each LP formed a through-hole was counted. The average value and the standard deviation of the drilling depth for each amount of laser energy were obtained as presented in Fig. 5, which shows that the drilling

Fig. 3 SEM images and depth profiles of craters formed on a Metglas foil by (a) 1 NSP and (b) 10 NSPs. Laser intensity was 20 mJ/pulse. The discontinuous points of the depth profile curves are caused by the insufficient reflection of the probe light of the three-dimensional interferometer from near-vertical surfaces

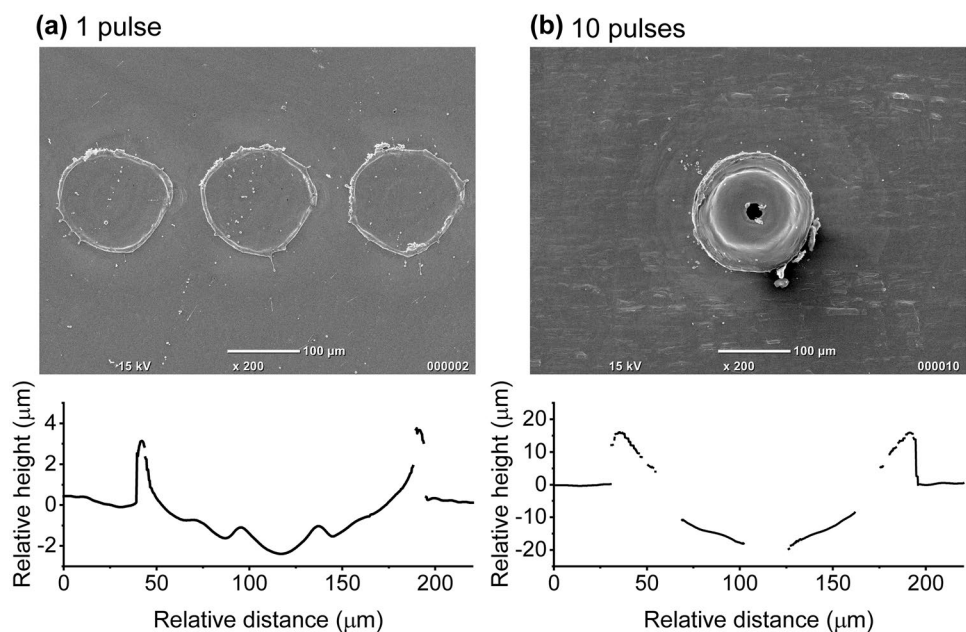
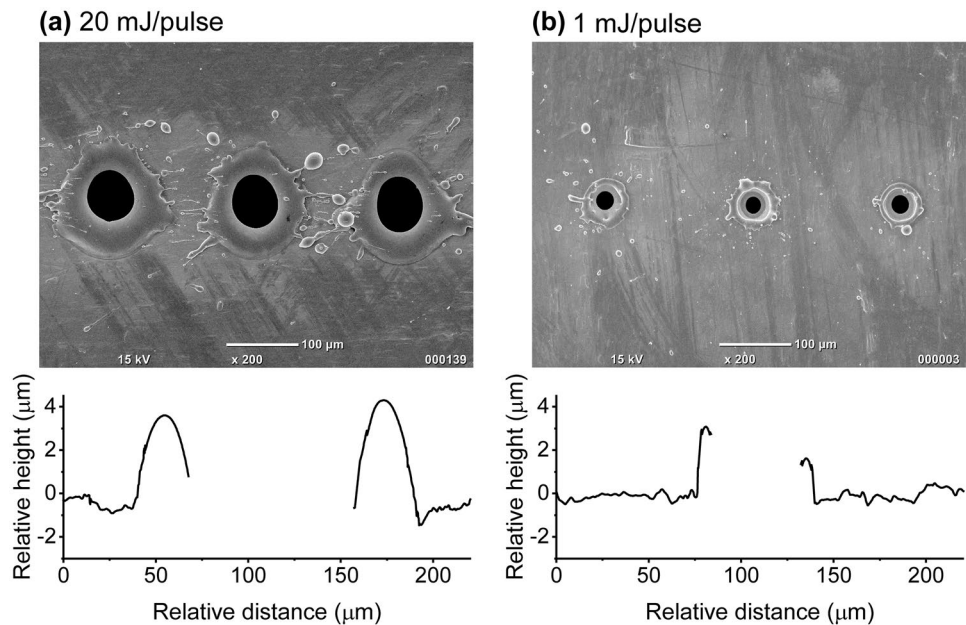


Fig. 4 SEM images and depth profiles of holes formed on a Metglas foil by LP mode pulses. Laser intensity was (a) 20 mJ/pulse and (b) 1 mJ/pulse. The discontinuous points of the depth profile curves are caused by the insufficient reflection of the probe light of the three-dimensional interferometer from near-vertical surfaces



depth of an LP at 20 mJ is ca. 480 μm (ca. 19–20 layers of foil), indicating that the drilling depth of an LP is ca. 160 times greater than that of an NSP at 20 mJ. Additionally, when the drilling efficiencies (drilling depth per unit of laser energy) of an NSP at 20 mJ and an LP at 1 mJ are compared, the drilling efficiency of an LP at 1 mJ (ca. 75 $\mu\text{m}/\text{mJ}$) is ca. 500 times higher than that of an NSP at 20 mJ (ca. 0.15 $\mu\text{m}/\text{mJ}$)

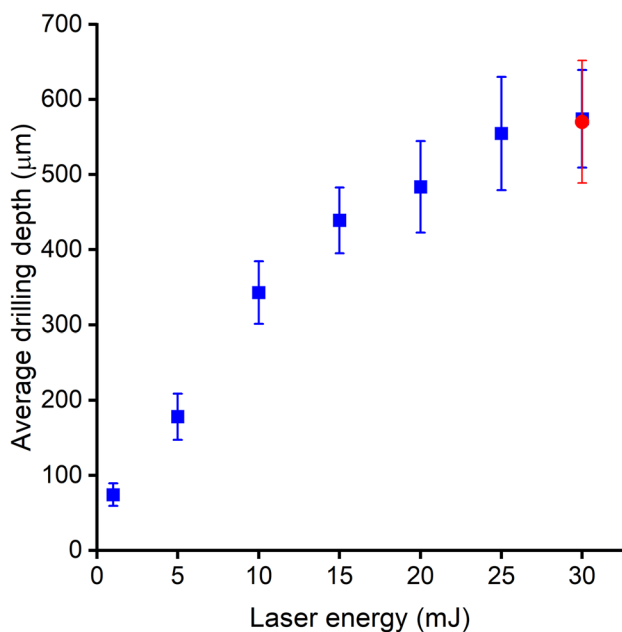


Fig. 5 Average drilling depth of an LP at various laser energies. The drilling depth was estimated by multiplying 25 μm by the number of foils on which an LP forms a through-hole. The red symbol at 30 mJ is the datum obtained when the focal position was set on the bottom layer

mJ). Figure 5 also shows that, although the drilling depth increased with increasing laser energy, the drilling efficiency of an LP becomes lower with energy greater than 15 mJ. We confirmed that this phenomenon is not attributable to the deviation of the focal condition because no significant difference of the average drilling depth was observed at 30 mJ when the focal point was set at the bottom layer.

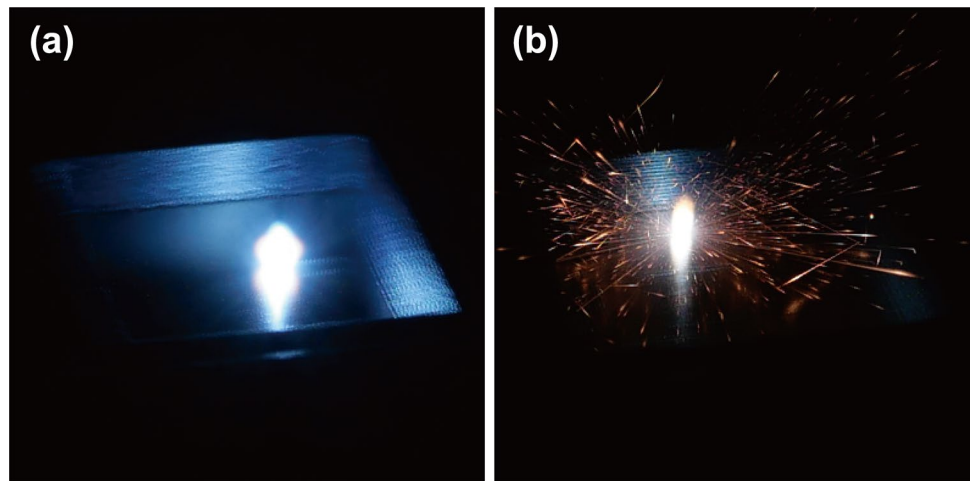
3.2 Mechanism of LP drilling

It is remarkable that the LP drilling efficiency is considerably higher than that of an NSP. We investigated what factors of LP irradiation bring this higher drilling efficiency.

As such a factor, the influence of plasma shielding was considered first because the appearance of a plasma plume observed during NPS irradiation and that observed during LP irradiation are vastly different (Fig. 6). When laser ablation of a metal target is done, plasma generated by the former part of a laser pulse is well known to absorb and reflects the latter part of the pulse, resulting in decreased ablation efficiency [18–20].

To investigate the influence of plasma shielding in the present case, optical emission spectra of laser-generated plasma plume were observed. As portrayed in Fig. 7, the optical emission intensity of plasma generated by an NSP at 20 mJ is significantly higher than that of plasma generated by an LP at 20 mJ. The higher optical emission intensity of plasma generated by an NSP will be attributable to the higher peak energy of an NSP than that of an LP. Consequently, plasma shielding will occur more efficiently for an NSP than for an LP, suggesting that the drilling efficiency of an NSP becomes lower than that of an LP. Additionally,

Fig. 6 Plasma plumes observed during irradiation of (a) NPSs and (b) LPs using a still camera. The still camera exposure time was 1 s. The laser and the still camera were not synchronized



the fact that the optical emission intensity of plasma generated by an LP increases with increasing laser intensity, as observed in Fig. 7, suggests that lowering of the drilling efficiency in the higher laser energy region of LP irradiation observed in Fig. 6 is attributable to the plasma shielding, indicating that the plasma shielding effect becomes prominent at higher energy, even when an LP is used. In other words, the use of lower energy is expected to be a key condition that enables us to carry out efficient drilling.

It can be proposed that the second important factor enhancing the drilling efficiency of LP irradiation is the characteristic temporal laser pulse profile of an LP. As presented in Fig. 1, an LP comprises many sub-pulses, meaning that laser energy is distributed on these sub-pulses. This feature contributes to suppression of the peak laser energy. Additionally, these sub-pulses

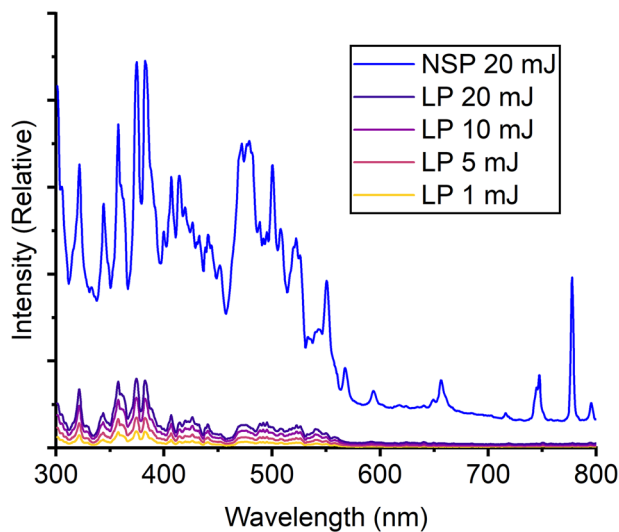


Fig. 7 Optical emission spectra of plasma generated using an NSP at 20 mJ and those generated using an LP at various energy. Each spectrum was obtained by averaging optical emissions of plasma generated by 10 laser shots

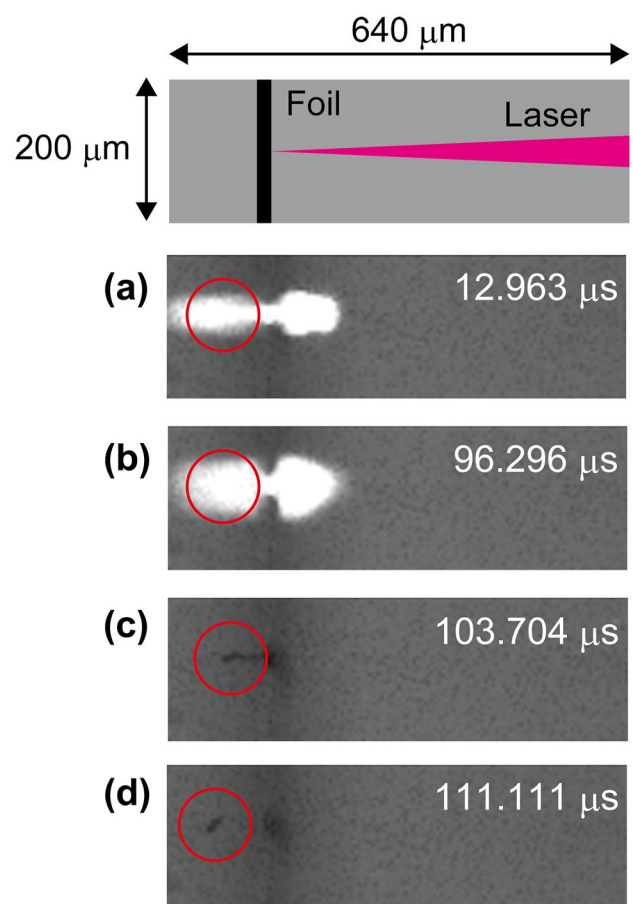
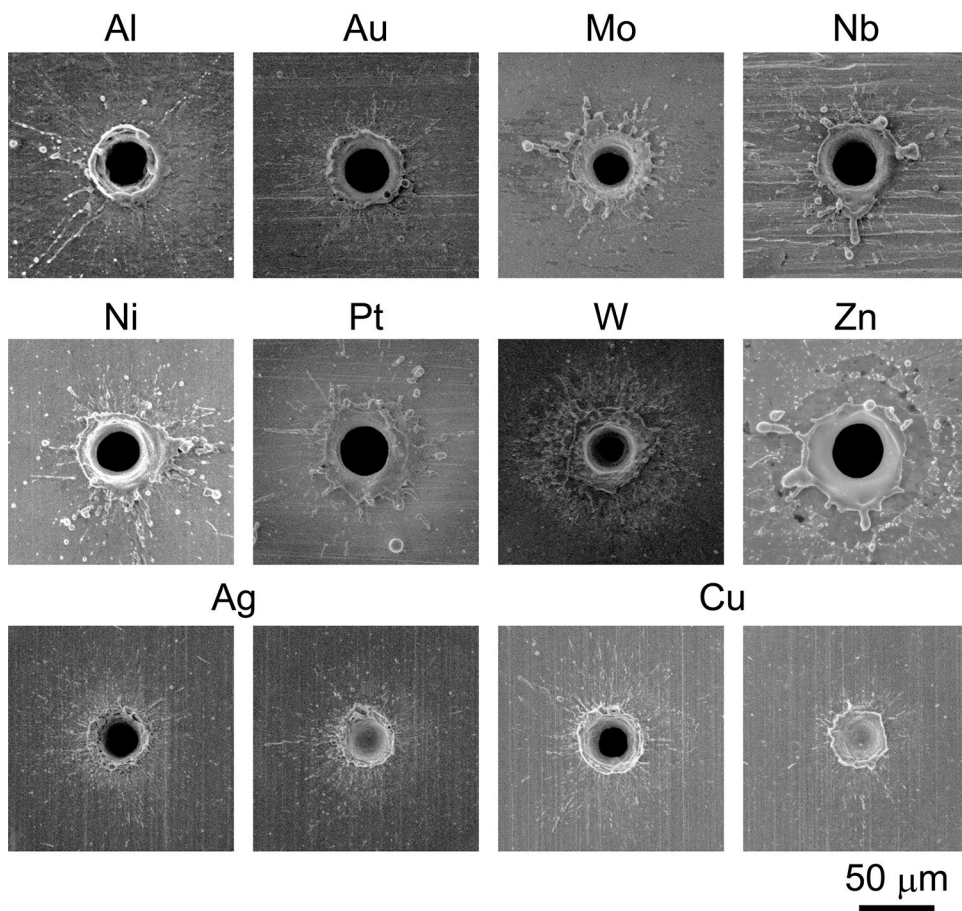


Fig. 8 High-speed camera images of laser ablation phenomena caused by laser irradiation of an LP at 2.5 mJ. The time shown in each photograph is the time from arrival of the first sub-pulse of an LP. Because of the difference between the camera frame rate ($540,000 \text{ s}^{-1}$) and the sub-pulse frequency (ca. $200,000 \text{ s}^{-1}$) in an LP, ablation phenomena caused by a several sub-pulses might be captured. The bright part marked by circles in (a) and (b) is assigned to the reflection of the optical emissions of plasma plume by the foil because of their symmetrical shape and comparisons with data obtained in an earlier study using thicker targets [17]

Fig. 9 Typical examples of holes formed on various metal foils by an LP at 5 mJ. The thicknesses of the foils are Ag: 30 mm, Al: 25 mm, Au: 30 mm, Cu: 25 mm, Mo: 25 mm, Nb: 25.4 mm, Ni: 30 mm, Pt: 30 mm, W: 30 mm, and Zn: 25 mm



might irradiate the same spot of the foil repeatedly [17], leading to promotion of drilling because the material heating occurs continuously. To investigate such a feature of the sub-pulse irradiation, high-speed camera observations were made of the laser ablation process caused by an LP. As shown in Fig. 8a, b, the optical emissions of plasma were observed several times during an LP irradiation. Additionally, the ejection of molten

matter was observed after the end of sub-pulses, as indicated by the circles in Fig. 8c, d. These results suggest that repeated irradiation of sub-pulses in an LP promotes the drilling.

We also applied low-energy LP drilling for various metal foils to investigate the versatility of this method. As shown in Fig. 9, in most cases, a through-hole was formed by the irradiation of an LP at 5 mJ, indicating this method as versatile. For

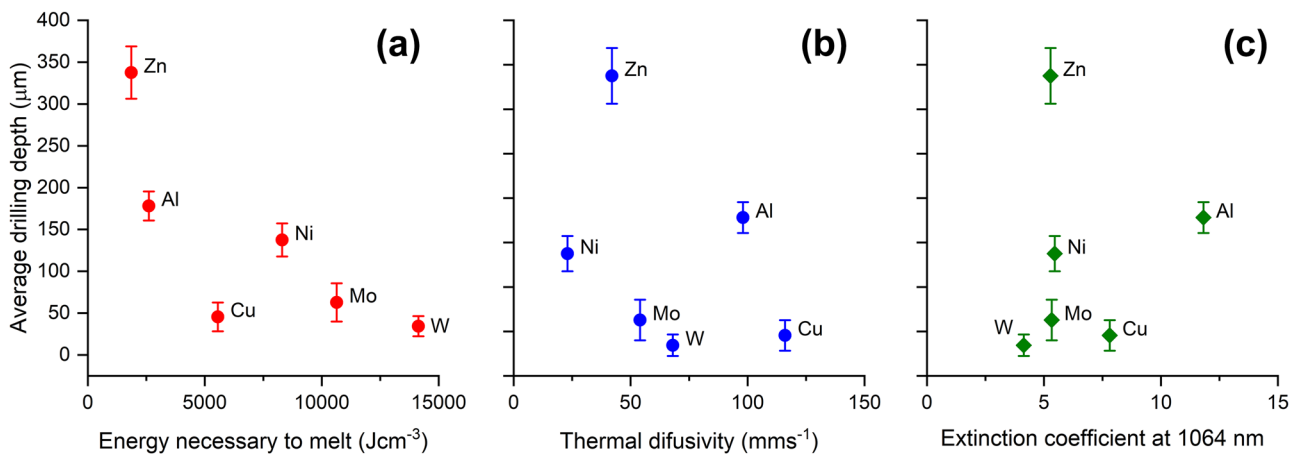


Fig. 10 Relation between the average depth of holes formed by irradiation of an LP at 5 mJ and (a) energy necessary to melt a material per unit volume, (b) thermal diffusivity, and (c) extinction coefficient

at 1064 nm. For Cu, some of the laser shots were unenabled to form a through-hole on the top foil as shown in Fig. 9. The values used for these analyses are listed in Table 1

Ag and Cu foils, some LP shots were unable to form a through-hole. Figure 9 also shows that the hole diameter depends on the metal species. These results suggest that some physical properties of the materials influence the drilling efficiency. To investigate such influences of materials properties on the drilling efficiency, we conducted the similar experiment to that to obtain the data shown in Fig. 5 and analyze the relation between the average drilling depth for a LP at 5 mJ and some physical properties of metals (energy necessary to melt a material per unit volume, thermal diffusivity, and extinction coefficient). The values used in these analyses are listed in Table 1. Here, the energy necessary to melt a material per unit volume (E_m) was obtained by using the following equation, where C_p is the specific heat capacity, T_m is the melting point, and ΔH_f is the enthalpy of fusion of each material.

$$E_m = C_p(T_m - 298) + \Delta H_f \quad (1)$$

The thermal diffusivity (α) was obtained by using the following equation, where l is the thermal conductivity and r is the density of each material.

$$\alpha = \frac{\lambda}{C_p \rho} \quad (2)$$

Figure 10a shows the relation between the energy necessary to a material and the average drilling depth. The drilling depth seems to correlate with this parameter except for Cu. This finding suggests that the drilling of an LP would proceed via melting of materials, which is consistent with the fact that the amount of plasma emission generated by an LP is small and is consistent with the morphology of the debris observed circumjacent to the holes. In such a thermal process, the temperature decrease in laser-irradiated portion due to the energy dispersion will also play an important role, particularly when long-pulse laser irradiation is used. As shown in Fig. 10b, although the drilling depth does not seem to correlate with this parameter, the lower drilling efficiency found for Cu can be explained based on their higher thermal diffusivity than those of other metals. It is suggested that the lower drilling efficiency found for Ag (Fig. 9) can be also interpreted as a result of the higher thermal diffusivity ($174 \text{ mm}^2/\text{s}$). Such an effect of the thermal diffusivity suggests that the balance of the plasma shielding effect and heat dispersion leads to the high drilling efficiency of an LP. In other words, the low-energy LP drilling is particularly suitable for materials with low E_m and α . From this viewpoint, it is suggested that the relatively lower melting point (ca. 1420–1470 K) and the relatively lower thermal conductivity ($7.74 \text{ Wm}^{-1} \text{ K}^{-1}$) of the amorphous alloy foil (Metglas) would enable us to use the LP drilling for this material efficiently.

4 Conclusion

Results of these experiments demonstrate that the use of an LP of a Nd:YAG laser is suitable for laser drilling of amorphous alloy foils. The drilling depth of an LP at 1 mJ was found to be ca. $75 \mu\text{m}$, although the drilling depth of the craters formed by an NSP at 20 mJ was ca. $3 \mu\text{m}$, indicating that the drilling efficiency of an LP at 1 mJ is ca. 500 times higher than that of a NSP at 20 mJ. Results suggest that such higher drilling efficiency is brought by the lower peak energy of an LP compared with that of a NSP because the lower peak energy of an LP reduces the plasma generation and plasma shielding, particularly at low energy. Results also suggest that the temporal profile of an LP contributes to efficient drilling: An LP comprising sub-pulses engenders a decrease in the peak energy of an LP; and repeated irradiation of the same portion of a foil by sub-pulses promotes drilling due to the continuous heating. Laser drilling using a low-energy LP was demonstrated as applicable to various metal foils, although the drilling efficiency depends on the metal species. The results of the analysis of the relation between the energy necessary to melt the metals and the drilling efficiency suggested that the drilling would proceed via melting of materials. Additionally, the influence of the thermal diffusivity on the drilling efficiency observed for some metals suggests that thermodynamic analysis must be conducted to understand the LP drilling process more precisely.

Acknowledgements The authors thank Dr. Nobuhiko Chiwata (Hitachi Metals Ltd.) for providing useful comments and information. We also thank Prof. Hidetoshi Miyazaki (Shimane University) for allowing us to use SEM. This work was supported by the project, “Subsidy for Regional University/Regional Industry Creation” of the Cabinet Office, Government of Japan: “Creation of a Global Base for Advanced Metals—Next Generation TATARA Project.”

Author contributions T.T., M.O., and D.N. conceived of the presented idea. T.T., M.O., D.N., S.Y., S.I., and H.H. carried out the experiments. T.T. wrote the manuscript with support from M.O. and D.N.

Funding The authors declare that no funds, grants, or other support were received during the preparation of this manuscript.

Availability of data and materials The datasets during and/or analyzed during the current study available from the corresponding author on reasonable request.

Declarations

Ethics approval Not applicable.

Consent to participate Not applicable.

Consent for publication Not applicable.

Competing interests The authors have no relevant financial or non-financial interests to disclose.

References

1. Tseng S-F, Liao C-H (2020) *Appl Surf Sci* 512
2. Tseng S-F, Huang CC (2021) *Appl Surf Sci* 570
3. Tseng S-F, Liao C-H, Hsiao W-T, Chang T-L (2021) *Ceram Int* 47:20
4. Glass JM, Groger HP, Churchill RJ, Norin EM (1990) *J Mater Eng* 12:1
5. Fujita K, Morishita Y, Nishiyama N, Kimura H, Inoue A (2005) *Mater Trans* 46:12
6. Knowles MRH, Rutterford G, Karnakis D, Ferguson A (2007) *Int J Adv Manuf Technol* 33:1–2
7. Williams E, Lavery N (2017) *J Mater Process Technol* 247
8. Zhang L, Huang H (2019) *Int J Adv Manuf Technol* 100:1–4
9. Zhikharev AV, Bayankin VY, Bystrov SG, Orlova NA (2019) *J Surf Ingestig* 13:6
10. Semerok A, Chaleard C, Detalle V, Lacour JL, Mauchien P, Meynadier P, Nouvellon C, Salle P, Palianov P, Perdrix M, Petite G (1999) *Appl Surf Sci* 139
11. Meijer J, Du K, Gillner A, Hoffmann D, Kovalenko VS, Masuzawa T, Ostendorf A, Poprawe R, Schulz W (2002) *CIRP Ann* 51:2
12. Hambach N, Hartmann C, Keller S, Gillner A (2016) *J Laser Micro/Nano Eng* 11(2):192
13. Zhao W, Yu Z (2018) *Opt Lasers Eng* 105
14. Zhao W, Liu H, Shen X, Wang L, Mei X (2020) *Materials* 13:1
15. Wang XL, Lu PX, Dai NL, Li YH, Liao CR, Zheng QG, Liu L (2007) *Mater Lett* 61:21
16. Solana P, Kapadia P, Dowden J, Rodden WSO, Kudesia SS, Hand DP, Jones JDC (2001) *Optics Communications* 191:1–2
17. Tasaki R, Higashihata M, Suwa A, Ikenoue H, Nakamura D (2018) *Appl Phys A* 124:2
18. Singh RK, Narayan J (1990) *Phys Rev B* 41:13
19. Singh RK (1996) *J Electron Mater* 25:1
20. Aguilera JA, Aragón C, Peñalba F (1998) *Appl Surf Sci* 127–129

Publisher's Note Springer Nature remains neutral with regard to jurisdictional claims in published maps and institutional affiliations.